

Surface Topography of the p3 and p6 Annexin V Crystal Forms Determined by Atomic Force Microscopy

Ilya Reviakine, Wilma Bergsma-Schutter, Christine Mazères-Dubut, Natalia Govorukhina, and Alain Brisson¹

Department of Biophysical Chemistry, GBB, University of Groningen, Nijenborgh 4, 9747 AG Groningen, The Netherlands

Received February 16, 2000, and in revised form May 15, 2000

Annexin V is a member of a family of structurally homologous proteins sharing the ability to bind to negatively charged phospholipid membranes in a Ca²⁺-dependent manner. The structure of the soluble form of annexin V has been solved by X-ray crystallography, while electron crystallography of two-dimensional (2D) crystals has been used to reveal the structure of its membrane-bound form. Two 2D crystal forms of annexin V have been reported to date, with either p6 or p3 symmetry. Atomic force microscopy has previously been used to investigate the growth and the topography of the p6 crystal form on supported phospholipid bilayers (Reviakine *et al.*, 1998). The surface structure of the second crystal form, p3, is presented in this study, along with an improved topographic map of the p6 crystal form. The observed topography is correlated with the structure determined by X-ray crystallography. © 2000 Academic Press

Key Words: annexin V; atomic force microscopy; 2D crystals; supported phospholipid bilayers.

INTRODUCTION

Since its invention more than a decade ago (Binnig *et al.*, 1986), atomic force microscopy (AFM) has become an established tool for studying the structure and behavior of biological macromolecules (proteins, DNA, lipids) and their assemblies in close-to-native, aqueous environments (reviewed in Hansma and Hoh, 1994; Engel *et al.*, 1997; Shao *et al.*, 1996). A substantial amount of work has been done on preformed two-dimensional (2D) crystals of soluble and membrane proteins (Engel *et al.*, 1997; Müller *et al.*, 1997a,b; Scheuring *et al.*, 1999) and on 2D crystals grown on supported phospholipid bilayers (SPBs) *in situ* (Reviakine *et al.*, 1998; Zuber *et al.*,

2000). Noncrystalline preparations of soluble proteins have been studied as well—by imaging protein molecules adsorbed to the surface of mica (Yang *et al.*, 1994; Mou *et al.*, 1996) or specifically bound to an SPB (Mou *et al.*, 1995) or by employing cryo-AFM (Han *et al.*, 1995). The high quality of AFM images has afforded a comparison with X-ray atomic models in a number of cases (Schabert *et al.*, 1995; Müller *et al.*, 1995; Scheuring *et al.*, 1999).

Annexin V (reviewed in Demange *et al.*, 1994) is a member of a family of soluble proteins, which share structural homology as well as the ability to bind to membranes containing negatively charged phospholipids in a Ca²⁺-dependent manner (Seaton, 1996). This property has been used to form 2D crystals of annexin V on lipid monolayers spread at the air-water interface (Uzgiris and Kornberg, 1983; Brisson *et al.*, 1994, 1999a) in order to study the structure of its membrane-bound form by electron microscopy (EM). It has been known for a long time that annexin V can crystallize in two crystal forms—with either p3 or p6 symmetry (Mosser *et al.*, 1991; Voges *et al.*, 1994; reviewed in Brisson *et al.*, 1999b). The recent finding that 2D arrays of annexin V were directly responsible for some functional properties (manuscript in preparation) prompted us to further investigate the structural relationships between crystal forms. This study focuses on the topographical structures of these two crystal forms, comparing the topographic maps obtained by AFM with the 2D projection maps obtained by cryo-EM and the X-ray model of soluble annexin V. The dynamics of the crystallization process, and the transition between crystal forms, will be reported elsewhere.

MATERIALS AND METHODS

Materials

Lipids used in this study were purchased from Avanti Polar Lipids (Alabaster, AL). Other chemicals were purchased from Merck (Germany) or Sigma (St. Louis, MO). Water used in this

study was purified with a MilliQ water purification system (Millipore).

Expression and Purification of Rat Annexin V

The protein coding sequence of rat annexin V was excised from a pKK233-2-annexin V expression construct (a gift of B. Pepinsky, Biogen, and B. Seaton, Boston University) and cloned into the expression vector pGEF (a gift of D. Janssen, Groningen University; Schanstra *et al.*, 1993). *Escherichia coli* BL21(DE3) cells carrying the annexin V construct were grown in 1 l LB medium at 30°C until an OD₆₀₀ reached 1. Annexin V expression was then induced by addition of 0.4 mM IPTG and growth was continued for 16 h. The cells were harvested by centrifugation (10 min, 6 krpm, 4°C) and resuspended in 50 ml buffer containing 10 mM Tris, 1 mM EDTA, 1 mM β -mercaptoethanol, 0.01% NaN₃, 10% glycerol, pH 7.5. The cell suspension was sonicated at 4°C six times for 1 min and large debris were removed by centrifugation at 100 000g for 1 h at 4°C. The supernatant was collected and stored until use at -20°C. For purification, the crude extract was either concentrated by ultrafiltration with an Amicon membrane (cutoff 10 kDa) or fractionated by ammonium sulfate (50 to 80% saturation range). The concentrated fraction (15 ml) was applied in 1-ml fractions to a Sephadex G-100 column (1 × 30 cm) pre-equilibrated with buffer A (20 mM Tris-HCl, pH 8.0, 0.1% NaN₃) and eluted with the same buffer. The fractions containing annexin V, identified by SDS-PAGE, were pooled and applied on a MonoQ column (Pharmacia) pre-equilibrated with buffer A, which was developed with a linear NaCl gradient in buffer A. Rat annexin V eluted at approximately 160 mM NaCl. Aliquots were stored at -80°C. The yield was about 35 mg pure protein per liter of cell culture.

Sample Preparation

SPBs, containing 20–60 wt% dioleoylphosphatidylserine (DOPS) in a mixture with dioleoylphosphatidylcholine (DOPC), were prepared from sonicated unilamellar vesicles by depositing 100 μ l of freshly sonicated vesicle suspension (0.5 mg/ml lipid in buffer B containing 2 mM CaCl₂, 150 mM NaCl, 10 mM Hepes, 3 mM NaN₃, pH 7.4, onto freshly cleaved 12-mm mica discs (Metafix, Montdidier, France) glued to Teflon-coated ("BYTAC," Norton Performance Plastics Corp., Akron, OH) metal discs (Müller *et al.*, 1997c). After ~1 h incubation, excess vesicles were removed by washing the specimen extensively with buffer B. Annexin V was added to a final concentration of ~0.1 mg/ml and incubated for a further 30 min, after which the specimen was installed in the AFM.

Atomic Force Microscopy

Images were acquired in contact constant-force mode, using oxide sharpened silicon nitride tips mounted on cantilevers with a nominal force constant of 0.06 N/m, on a Nanoscope IIIa multimode AFM (Digital Instruments, CA) equipped with a 16- μ m ("E") scanner. Scanning rates were typically 8–15 Hz and the scan angle was 90°. The force was kept at the lowest possible value by continuously adjusting the set point during imaging. O-rings were not used.

Image Processing

High-resolution 200 × 200 nm images of the p3 crystal form were analyzed by single-particle averaging procedures (Frank, 1990) using Imagic software (van Heel and Keegstra, 1981). Individual motifs (see figure legends) were selected visually and extracted into 64 × 64 pixel (25 × 25 nm) subfiles. They were subjected to sequential alignment steps using one of the particles as a reference until the correlation coefficients stabilized. Images with the best correlation coefficients were summed. Threefold

rotational symmetry was imposed where appropriate (see figure legends).

The high-resolution topographic map of the annexin V p6 2D crystals was calculated from an AFM image using standard Fourier methods.

The procedures used for the formation of annexin V 2D crystals on phospholipid monolayers at an air-water interface and for their electron crystallography analysis are described in detail in Brisson *et al.* (1999a,b).

RESULTS AND DISCUSSION

In a previous paper (Reviakine *et al.*, 1998), the formation and the topography of the p6 crystal form of annexin V grown on lipid bilayers was discussed. Figure 1 presents the topography structure of another phase in which annexin V crystallizes, with p3 symmetry. An improved topographic map of the p6 crystal form (at 1.5 nm resolution) is presented on Fig. 2, along with a 2D projection map calculated from cryo-EM images (Brisson *et al.*, 1999b), to facilitate the comparison between the two crystal forms.

It is known from EM that both crystal forms are built up of annexin V trimers (Figs. 1E and 2B, trimers circled in green), which also constitute the basic building blocks of most 3D crystal forms (Brisson and Lewit-Bentley, 1996). Yet the AFM images of the two crystal forms are quite different (compare Figs. 1A–1C and 2A). Moreover, the images of the p3 crystals were found to be force-dependent, while those of the p6 ones were not. The images shown on Figs. 1A and 1B were recorded with a minimal force (~100 pN). Annexin V trimers are not resolved on them. An increase in the applied force leads to an image such as that shown on Fig. 1C, where the trimers become apparent (circled in green). From the analysis of the averaged topographic map (Fig. 1D) and the comparison with the EM 2D projection map (Fig. 1E) it is evident that the structures visible in Fig. 1B (blue circle and inset) are the trimer-trimer connections, made up by the domains 3 of the annexin V monomers (numbering according to Huber *et al.*, 1990). These motifs are circled in blue in Figs. 1B–1E and correspond to the centers of the triskelion motifs previously identified by EM (Mosser *et al.*, 1991). The fact that domains 3 appear higher than the rest of the trimer is consistent with our earlier results obtained on the p6 crystal form (Reviakine *et al.*, 1998, see also Fig. 2). The susceptibility of the protein loop present at the top of domain 3—namely, the loop connecting helices 2E and 3A (shown in green on Fig. 3)—to the applied force is the likely reason for the force-induced change in the appearance of the p3 crystals (Müller *et al.*, 1997b).

The assertion that the loop connecting helices 2E and 3A above domain 3 is the highest point of the molecule agrees well with the X-ray structure of

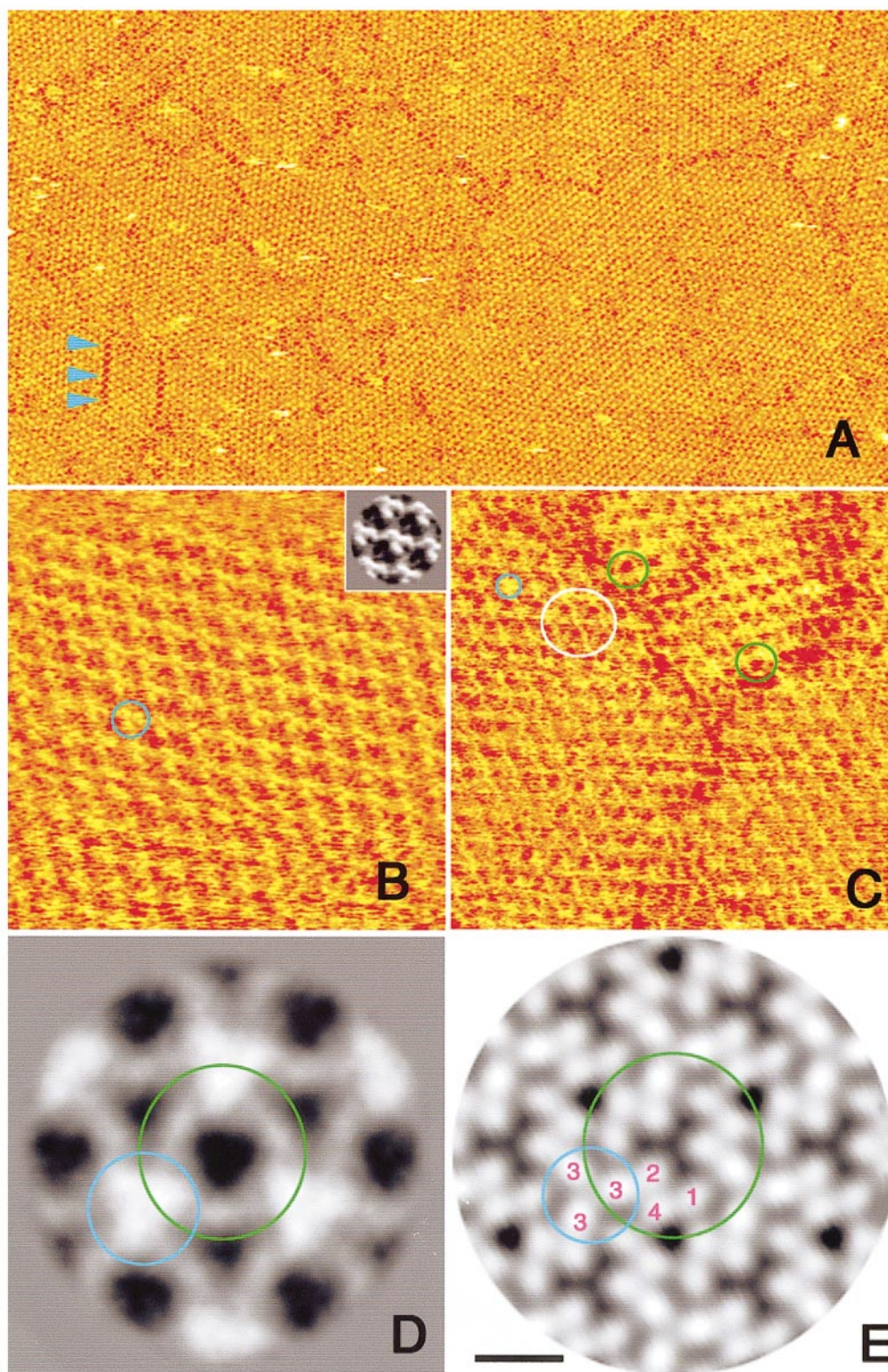


FIG. 1. p3 crystal form of annexin V. (A) An overview AFM image of the p3 crystal form. Image size (Z-scale): $1.5 \times 0.75 \mu\text{m}$ (3 nm). One of the many defects visible is marked with blue arrowheads. (B and C) The AFM images of the p3 form varied in appearance, depending on the applied force, as shown in (B) (minimal force) and (C) (higher force). The process was reversible (not shown). Scan size (Z-scale), nm: 116 (3), 145 (2.5). (B, inset) An averaged topographic map calculated by selecting 72 (25×25 nm) areas centered on motifs such as the one circled in blue, aligning them, and summing 16 images with the highest correlation coefficients (see Materials and

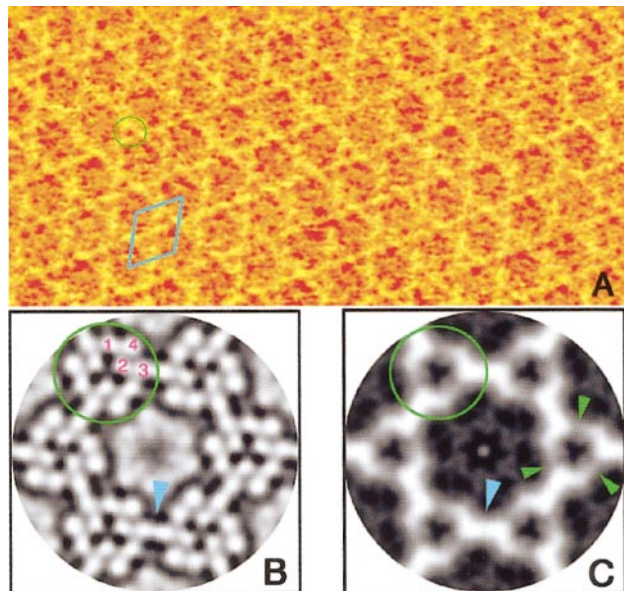


FIG. 2. p6 crystal form of annexin V. (A) An AFM image of the p6 crystal form used to calculate the topographic map shown in (C). Image size (Z-scale): 250×125 (2.5) nm. The image was low pass filtered to remove high-frequency noise components. The $a = b = 19.8 \pm 1$ nm, $\gamma = 120 \pm 0.4^\circ$ unit cell is marked with a blue lozenge. An annexin V trimer is circled in green. (B) 2D projected structure of membrane-bound annexin V at 1.5 nm resolution, calculated by cryoelectron crystallography of a p6 2D crystal grown on a lipid monolayer at the air–water interface, and transferred to an EM grid coated with a perforated carbon film (Brisson *et al.*, 1999b). Annexin V molecules are viewed from the aqueous solution. One trimer is circled in green. The four domains making up an annexin V monomer are indicated. The connecting region between the trimers, made by domains 3, is indicated with a blue arrow for comparison with the p3 form. Image size, 36×36 nm. (C) Average topographic map of the p6 crystal form of annexin V grown on a DOPC:DOPS SPB calculated by Fourier methods from the image shown in (A) at 1.5 nm resolution. A trimer is circled in green. The blue arrow indicates the connection between two adjacent trimers, for comparison with the p3 crystal form. This region undergoes changes between the p6 and the p3 crystal forms. The topographically lower region corresponding to domain 1 and its junction with the (3,2) module is pointed to by three green arrowheads for comparison with the X-ray map shown in Fig. 3. Image size, 35×35 nm.

annexin V shown on Fig. 3. The rest of the density corresponding to the surface of domain 3 (Fig. 2C) is defined by helix 3C (shown in yellow in Fig. 3). The

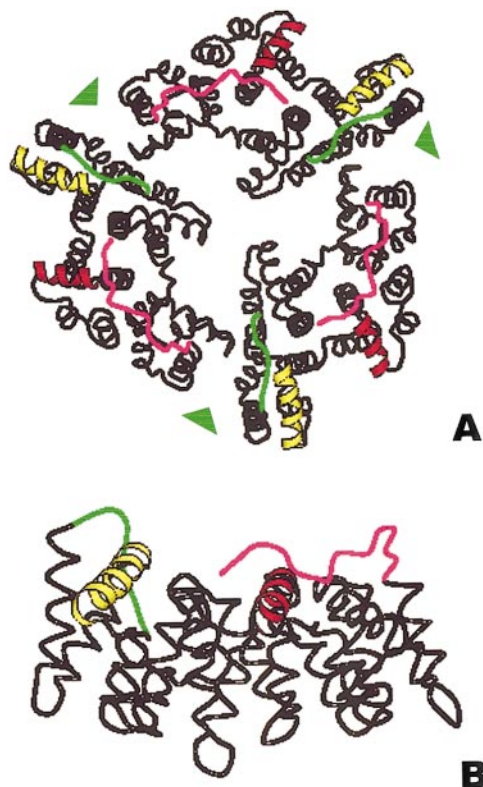


FIG. 3. Backbone models of annexin V trimer (A, viewed in the same orientation as the AFM images) and monomer (B, viewed from the side), generated from the X-ray structure by Sopkova *et al.* (1993). The loop connecting helices 2E and 3A (highlighted in green, numbering according to Huber *et al.* (1990) is at the very top of the molecule. Together with helix 3C (yellow), located somewhat below this loop, these structures define the surface of domain 3 as imaged by AFM. The N-terminal segment (purple), which is extended over the (1,4) module, together with helix 4C (red) defines the shape of the region corresponding to domain 4 on the AFM topographic map. Green arrowheads (in A) point to the topographically lower region between domain 1 and the (3,2) module (see Fig. 2C).

region corresponding to domain 4 (compare Figs. 2B and 2C) is the next highest. The features which contribute to its appearance on the AFM map are the N-terminal segment of the molecule (shown in purple in Fig. 3), which extends from helix 4E above

Methods). The inherently high contrast of the AFM images compensates for the small number of images summed. A corresponding motif is also circled in blue in (C). In both images, this motif protrudes above the rest of the structure. It is surrounded by three annexin V trimers—an arrangement circled in white. Green circles identify annexin V trimers. The Fourier transform of the image shown in (B) exhibited peaks extending up to 1.6 nm. The average lattice constant of the p3 crystal form was 9.2 ± 0.3 nm. (D) Average topographic map of the p3 crystal form obtained by single particle averaging from the image shown in (C). After summing 60 of the 200 (25×25 nm) aligned images, threefold symmetry was imposed on the structure. (E) 2D projected structure of the p3 form of membrane-bound annexin V at 2.4 nm resolution, calculated from EM images of negatively stained 2D crystals grown on a lipid monolayer at the air–water interface, and transferred to a carbon-coated EM grid (Mosser *et al.*, 1991). The domains of an annexin V molecule are numbered according to Huber *et al.* (1990). The center of the triskelion motif formed by the domains 3 of the three adjacent annexin V trimers is circled in blue and corresponds to the motif observed by AFM (blue circles in B–D). One trimer is circled in green. Scale bar, 5 nm.

domain 4 toward domain 1, and the helix 4C (shown in red in Fig. 3), which extends toward the periphery of domain 4. Yet lower on the AFM topographic map is the area corresponding to the junction between domain 1 and the (3,2) module of the adjacent monomer, consistent with the X-ray model (green arrowheads in Figs. 2C and 3).

In spite of the increased resolution of the AFM images of the p6 crystal form, domain 2 is not visible on the averaged topographic map (Fig. 2C). It is also absent on the AFM images of the p3 form, confirming the earlier assertion that topographically it is the lowest of the four domains (Reviakine *et al.*, 1998). The overall shape of the trimer suggested by AFM—sloping toward the interior of the trimer, away from domain 3—resembles that observed on the X-ray model (Sopkova *et al.*, 1993).

Conclusions

The observation that annexin V forms two distinct crystal forms on lipid monolayers has been extended in this work to supported phospholipid bilayers. The topography of both crystal forms as determined by AFM compares favorably with the 3D structure solved by X-ray crystallography and the 2D projection structures obtained by electron crystallography.

We thank Dr. B. Pepinsky, Dr. B. Seaton, and D. Janssen for their generous gifts of the annexin V cDNA and the pGEF expression vector, respectively. We greatly acknowledge Dr. J. Sopkova for providing us with an atomic model of annexin V trimer and for the realization of Fig. 3. I.R. is the recipient of a Ubbo Emmius Ph.D. fellowship from the University of Groningen. This work was supported by EC Grants BI04-98-0110 and BI04-98-0543 to A.B.

REFERENCES

- Binnig, G., Quate, C. F., and Gerber, Ch. (1986) Atomic force microscope, *Phys. Rev. Lett.* **56**(9), 930–933.
- Brisson, A., Lambert, O., and Bergsma-Schutter, W. (1999a) in Ducruix, A., and Giegé, E. (Eds.), *Crystallization of Nucleic Acids and Proteins: A Practical Approach*, pp. 342–363, Oxford Univ. Press, New York.
- Brisson, A., Bergsma-Schutter, W., Oling, F., Lambert, O., and Reviakine, I. (1999b) *J. Cryst. Growth* **196**, 456–470.
- Brisson, A., and Lewit-Bentley, A. (1996) in Seaton, B. A. (Ed.), *Annexins: Molecular Structure to Cellular Function*, pp. 43–52, Chapman & Hall, New York.
- Brisson, A., Olofsson, A., Ringler, P., Schmutz, M., and Stoylova, S. (1994) Two-dimensional crystallisation of proteins on planar lipid films and structure determination by electron crystallography, *Biol. Cell* **80**, 221–228.
- Demange, P., Voges, D., Benz, J., Liemann, S., Gottig, P., Berendes, R., Burger, A., and Huber, R. (1994) Annexin V: The key to understanding ion selectivity and voltage regulation, *Trends Biochem. Sci.* **19**, 272–276.
- Engel, A., Schoenenberger, C.-A., and Müller, D. J. (1997) High resolution imaging of native biological sample surfaces using scanning probe microscopy, *Curr. Opin. Struct. Biol.* **7**, 279–285.
- Frank, J. (1990) Classification of macromolecular assemblies studied as single particles, *Q. Rev. Biophys.* **23**, 281–329.
- Han, W., Mou, J., Sheng, J., Yang, J., and Shao, Z. (1995) Cryo atomic force microscopy: A new approach for biological imaging at high resolution, *Biochemistry* **34**, 8215–8220.
- Hansma, H. G., and Hoh, J. H. (1994) Biomolecular imaging with the atomic force microscope, *Annu. Rev. Biophys. Biomol. Struct.* **23**, 115–139.
- van Heel, M. G., and Keegstra, W. (1981) IMAGIC: A fast, flexible and friendly image analysis system, *Ultramicroscopy* **7**, 113–130.
- Huber, R., Römisch, J. M., and Paques, E. P. (1990) The crystal and molecular structure of human annexin V, an anticoagulant protein that binds to calcium and membranes, *EMBO J.* **9**, 3867–3874.
- Mosser, G., Ravanat, C., Freyssinet, J.-M., and Brisson, A. (1991) Sub-domain structure of lipid-bound annexin-V resolved by electron image analysis, *J. Mol. Biol.* **217**, 241–245.
- Mou, J., Yang, J., and Shao, Z. (1995) Atomic force microscopy of cholera toxin B-oligomers bound to bilayers of biologically relevant lipids, *J. Mol. Biol.* **248**, 507–512.
- Mou, J., Czajkowsky, D. M., Shang, S. J., Ho, R., and Shao, Z. (1996) High resolution surface structure of E.coli GroES oligomer by atomic force microscopy, *FEBS Lett.* **381**, 161–164.
- Müller, D. J., Schabert, F. A., Büldt, G., and Engel, A. (1995) Imaging purple membranes in aqueous solutions at sub-nanometer resolution by atomic force microscopy, *Biophys. J.* **68**, 1681–1686.
- Müller, D., Engel, A., Carrascosa, J. L., and Velez, M. (1997a) The bacteriophage ϕ 29 head-tail connector imaged at high resolution with the atomic force microscope in buffer solution, *EMBO J.* **10**, 2547–2553.
- Müller, D. J., Schoenenberger, C.-A., Schabert, F., and Engel, A. (1997b) Structural changes in native membrane proteins monitored at subnanometer resolution with the atomic force microscope: A review, *J. Struct. Biol.* **121**, 149–157.
- Müller, D. J., Amrein, M., and Engel, A. (1997c) Adsorption of biological macromolecules to a solid support for scanning probe microscopy, *J. Struct. Biol.* **119**, 172–188.
- Reviakine, I., Bergsma-Schutter, W., and Brisson, A. (1998) Growth of protein 2-D crystals on supported planar lipid bilayers imaged *in situ* by AFM, *J. Struct. Biol.* **121**, 356–361.
- Schabert, F. A., Henn, C., and Engel, A. (1995) Native *Escherichia coli* OmpF porin surfaces probed by atomic force microscopy, *Science* **268**, 92–94.
- Schanstra, J. P., Rink, R., Pries, F., and Janssen, D. B. (1993) Construction of an expression and site-directed mutagenesis system of haloalkane dehalogenase in *Escherichia coli*, *Protein Expression Purif.* **4**, 479–489.
- Scheuring, S., Müller, D. J., Ringler, P., Heymann, J. B., and Engel, A. (1999) Imaging streptavidin 2D crystals on biotinylated lipid monolayers at high resolution with the atomic force microscope, *J. Microsc.* **193**, 28–35.
- Seaton, B. A. (1996) *Annexins: Molecular Structure to Cellular Function* Chapman & Hall, New York.
- Shao, Z., Mou, J., Czajkowsky, D. M., Yang, J., and Yuan, J.-Y. (1996) Biological atomic force microscopy: What is achieved and what is needed, *Adv. Phys.* **45**, 1–86.
- Sopkova, J., Renouard, M., and Lewit-Bentley, A. (1993) The crystal structure of a new high-calcium form of annexin V, *J. Mol. Biol.* **234**, 816–825.
- Uzgriris, E. E., and Kornberg, R. D. (1983) Two-dimensional crystallization technique for imaging macromolecules, with appli-

- cation to antigen-antibody-complement complexes, *Nature* **301**, 125–129.
- Voges, D., Berendes, R., Burger, A., Demange, P., Baumeister, W., and Huber, R. (1994) Three-dimensional structure of membrane bound annexin V—A correlative electron microscopy-X-ray crystallography study, *J. Mol. Biol.* **238**, 199–213.
- Yang, J., Mou, J., and Shao, Z. (1994) Structure and stability of pertussis toxin studied by in situ atomic force microscopy, *FEBS Lett.* **338**, 89–92.
- Zuber, G., and Barklis, E. (2000) Atomic force microscopy and electron microscopy analysis of retrovirus Gag proteins assembled in vitro on lipid bilayers, *Biophys. J.* **78**, 373–384.